HHS Public Access

Author manuscript

Exp Eye Res. Author manuscript; available in PMC 2023 January 01.

Published in final edited form as:

Exp Eye Res. 2022 January ; 214: 108866. doi:10.1016/j.exer.2021.108866.

Melanopsin modulates refractive development and myopia

Ranjay Chakraborty[a,b,c,d], **Erica G. Landis**[a,b,e], **Reece Mazade**[b,f], **Victoria Yang**[b,f], **Ryan Strickland**[b,e], **Samer Hattar**[g], **Richard A. Stone**[h], **P. Michael Iuvone**[a,i], **Machelle T. Pardue**[b,e,f]

[a]Department of Ophthalmology, Emory University School of Medicine, 1365B Clifton Rd NE, Atlanta, GA 30322, United States

[b]Center for Visual and Neurocognitive Rehabilitation, Atlanta VA Health Care System, 1670 Clairmont Rd, Decatur, GA 30033, United States

[c]College of Nursing and Health Sciences, Optometry and Vision Science, Flinders University, Bedford Park, SA 5001, Adelaide, Australia

[d]Caring Futures Institute, Flinders University, Bedford Park, SA 5042, Adelaide, Australia

[e]Neuroscience Program, Emory University School of Medicine, 1365 Clifton Rd NE, Atlanta, GA 30322, United States

[f]Department of Biomedical Engineering, Georgia Institute of Technology, 313 Ferst Dr, Atlanta, GA 30332, United States

[g]Section on Light and Circadian Rhythms, NIMH, NIH, 9000 Rockville Pike, Bethesda, Maryland, USA 20892

[h]Department of Ophthalmology, University of Pennsylvania Perelman School of Medicine, Philadelphia, Pennsylvania, United States

[i]Department of Pharmacology, Emory University School of Medicine, 1365B Clifton Rd NE, Atlanta, GA 30322, United States

Abstract

Myopia, or nearsightedness, is the most common form of refractive abnormality and is characterized by excessive ocular elongation in relation to ocular power. Retinal neurotransmitter signaling, including dopamine, is implicated in myopic ocular growth, but the visual pathways that initiate and sustain myopia remain unclear. Melanopsin-expressing retinal ganglion cells

Corresponding Author Machelle T. Pardue, PhD, Research Service (151 Oph), Atlanta VA Healthcare System, 1670 Clairmont Rd., Decatur, GA 30033, Ph: 404-321-6111 X207342, machelle.pardue@bme.gatech.edu.

Author Contributions: RC conceived the project, performed experiments, analyzed data, wrote and revised the manuscript; EGL performed experiments, analyzed data, wrote and revised the manuscript; RM analyzed data, wrote and revised the manuscript; VY performed experiments and analyzed data; RS performed experiments and analyzed data; SH conceived the project and revised the manuscript; RAS conceived the project and revised the manuscript; PMI conceived the project and revised the manuscript; MTP conceived the project, analyzed data, wrote and revised the manuscript.

Disclosures: R. Chakraborty, None; E.G. Landis, None; R. Mazade, None; V. Yang, None; R. Strickland, None; S. Hattar, None; R.A. Stone, None; P.M. Iuvone, None; M.T. Pardue, None

(mRGCs), which detect light, are important for visual function, and have connections with retinal dopamine cells. Here, we investigated how mRGCs influence normal and myopic refractive development using two mutant mouse models: *Opn4*$^{-/-}$ mice that lack functional melanopsin photopigments and intrinsic mRGC responses but still receive other photoreceptor-mediated input to these cells; and *Opn4*$^{DTA/DTA}$ mice that lack intrinsic and photoreceptor-mediated mRGC responses due to mRGC cell death. In mice with intact vision or form-deprivation, we measured refractive error, ocular properties including axial length and corneal curvature, and the levels of retinal dopamine and its primary metabolite, L-3,4-dihydroxyphenylalanine (DOPAC). Myopia was measured as a myopic shift, or the difference in refractive error between the form-deprived and contralateral eyes. We found that *Opn4*$^{-/-}$ mice had altered normal refractive development compared to *Opn4*$^{+/+}$ wildtype mice, starting ~4D more myopic but developing ~2D greater hyperopia by 16 weeks of age. Consistent with hyperopia at older ages, 16 week-old *Opn4*$^{-/-}$ mice also had shorter eyes compared to *Opn4*$^{+/+}$ mice (3.34 vs 3.42 mm). *Opn4*$^{DTA/DTA}$ mice, however, were more hyperopic than both *Opn4*$^{+/+}$ and *Opn4*$^{-/-}$ mice across development ending with even shorter axial lengths. Despite these differences, both *Opn4*$^{-/-}$ and *Opn4*$^{DTA/DTA}$ mice had ~2D greater myopic shifts in response to form-deprivation compared to *Opn4*$^{+/+}$ mice. Furthermore, when vision was intact, dopamine and DOPAC levels were similar between *Opn4*$^{-/-}$ and *Opn4*$^{+/+}$ mice, but higher in *Opn4*$^{DTA/DTA}$ mice, which differed with age. However, form-deprivation reduced retinal dopamine and DOAPC by ~20% in *Opn4*$^{-/-}$ compared to *Opn4*$^{+/+}$ mice but did not affect retinal dopamine and DOPAC in *Opn4*$^{DTA/DTA}$ mice. Lastly, systemically treating *Opn4*$^{-/-}$ mice with the dopamine precursor L-DOPA reduced their form-deprivation myopia by half compared to non-treated mice. Collectively our findings show that disruption of retinal melanopsin signaling alters the rate and magnitude of normal refractive development, yields greater susceptibility to form-deprivation myopia, and changes dopamine signaling. Our results suggest that mRGCs participate in the eye's response to myopigenic stimuli, acting partly through dopaminergic mechanisms, and provide a potential therapeutic target underling myopia progression. We conclude that proper mRGC function is necessary for correct refractive development and protection from myopia progression.

Keywords

Opn4; Melanopsin retinal ganglion cells (mRGCs); Dopamine; 3,4-dihydroxyphenylacetic acid (DOPAC); L-3,4-dihydroxyphenylalanine (L-DOPA)

1. Introduction

Melanopsin-expressing retinal ganglion cells (mRGCs) are subtypes of ganglion cells that act as photoreceptors (Berson et al., 2002; Hattar et al., 2002). mRGCs respond to light directly through melanopsin, a blue-light sensitive photopigment (Hattar et al., 2002), and indirectly through synaptically-mediated input from rod and cone photoreceptors (Sand et al., 2012; Schmidt et al., 2011a; Schmidt et al., 2011b). Though mRGCs comprise only 0.2 – 2.5% of all retinal ganglion cells across species (Dacey et al., 2005; Hattar et al., 2002), they are involved in diverse functions including photoentrainment of circadian rhythms, pupillary light reflex, sleep, and alertness (Berson et al., 2002; Hatori et al., 2008; Hattar et al., 2006; Panda et al., 2002) as well as contrast and color detection (Schmidt et al., 2014; Zele et

al., 2018), and pattern vision (Ecker et al., 2010). In addition, impaired mRGC function is associated with multiple ocular diseases (Feigl and Zele, 2014). However, it is unknown if or how mRGC signaling influences refractive development of the eye.

Myopia is the most common refractive error and primarily results from excessive elongation of the eye relative to its optical power. Myopia is a leading cause of visual impairment because of its association with a number of eye diseases such as retinal tear and detachment, glaucoma, and cataracts (Sankaridurg et al., 2021; Saw, 2006). Although an extensive literature implicates genetic and environmental influences on myopia development (Morgan, 2003; Mutti et al., 2002; Rose et al., 2008), the underlying mechanisms remain elusive. Therefore, we investigated the role of melanopsin-mediated signaling in refractive development and myopia susceptibility in the mouse.

mRGCs represent a potential candidate for influencing refractive development and myopia due to their morphological and functional diversity, connectivity with other inner retinal neurons, and role in image and non-image forming functions. For example, retinal dopaminergic amacrine cell processes and mRGC dendrites colocalize (Dumitrescu et al., 2009; Vugler et al., 2007) and there is strong morphological and electrophysiological evidence for synaptic drive of dopaminergic amacrine cells by mRGCs (Dumitrescu et al., 2009; Grunert et al., 2011; Hoshi et al., 2009; Prigge et al., 2016; Zhang et al., 2008; Zhao et al., 2017), although this input may not drive global retinal dopamine release (Cameron et al., 2009; Munteanu et al., 2018). Retinal dopamine is critical in regulating ocular growth and myopia (Feldkaemper and Schaeffel, 2013; Troilo et al., 2019; Zhou et al., 2017). In chicks and mammals, including primates, development of experimentally induced form-deprivation (FD) myopia is associated with lower levels of retinal dopamine (DA), and its primary metabolite 3,4-dihydroxyphenylacetic acid (DOPAC) (Iuvone et al., 1989; McBrien et al., 2001; Stone et al., 1989). In addition, administration of DA receptor agonists (Ashby et al., 2007; Dong et al., 2011; Iuvone et al., 1991; McCarthy et al., 2007; Rohrer et al., 1993; Stone et al., 1989), or the DA precursor, L-3,4-dihydroxyphenylalanine (L-DOPA) (Landis et al., 2020; Mao et al., 2010; Thomson et al., 2020), significantly inhibits the development of FD myopia in animals. mRGCs also contribute to visual detection and contrast processing (Schmidt et al., 2014; Zele et al., 2018) that could modulate the direction of eye growth and refractive development (Schmid and Wildsoet, 1997). Moreover, use of a melanopsin signaling antagonist in guinea pigs slightly inhibited lens-induced myopia (Zheng et al., 2020). Furthermore, mRNA expression of the melanopsin encoding gene, *Opn4*, in the chick retina is altered after lens-induced experimental myopia (Stone et al., 2011a) and the diurnal oscillation of melanopsin mRNA is perturbed in experimental models of myopia and hyperopia (Stone et al., 2020). Together, these results suggest melanopsin signaling is likely important in ocular growth and development of myopia.

To investigate the role of mRGC-mediated pathways on refractive development and myopia susceptibility, we employed two different mouse models: 1. $Opn4^{-/-}$ mice that lack intrinsic mRGC light responses due to a null mutation in *Opn4* (Panda et al., 2002) but still mediate rod and cone photoreceptor signaling through the mRGCs and 2. $Opn4^{DTA/DTA}$ mice that have genetically ablated mRGC cell bodies resulting in the absence of intrinsic mRGC responses and synaptic input from rod-cone networks to these cells (Guler et al., 2008).

We hypothesized that the absence of melanopsin photopigment in *Opn4*$^{-/-}$ mice would alter normal refractive development and increase susceptibility to FD myopia (Pardue et al., 2013). We also hypothesized that *Opn4*$^{DTA/DTA}$ mice would exhibit a more severe refractive phenotype due to the total loss of signaling through mRGCs. Furthermore, we tested the potential interaction of DA and mRGCs by measuring retinal DA levels, hypothesizing that a lack of functional mRGCs will reduce levels of DA and DOPAC, and that treating *Opn4*$^{-/-}$ mice with L-DOPA will favorably affect myopia progression. Lastly, we evaluated morphological changes in mRGCs and dopaminergic amacrine cells in FD.

2. Materials and methods

2.1 Animals

All experiments were approved by the local Institutional Animal Care and Use Committee and adhered to the ARVO statement for the Use of Animals in Ophthalmic and Vision Research. Refractive development and myopia susceptibility were measured in two mutant mouse models: *Opn4*$^{-/-}$ and *Opn4*$^{DTA/DTA}$ mice (both gifts from Dr. Samer Hattar, Johns Hopkins University, Baltimore, United States). *Opn4*$^{-/-}$ mice have no melanopsin-mediated light response due to the absence of melanopsin photopigment (Panda et al., 2002; Ruby et al., 2002). *Opn4*$^{-/-}$ mice exhibit diminished pupillary light reflex (PLR) (Lucas et al., 2003) and deficits in circadian photoentrainment (Panda et al., 2002; Ruby et al., 2002), without any apparent anatomical or developmental ocular defects (Panda et al., 2002). A single nucleotide polymorphism (SNP) genome scanning analysis from the Jackson Laboratory (Bar Harbor, ME) revealed *Opn4*$^{-/-}$ mice to be approximately 60% 129S1/SvImJ (129J) and 40% C57BL/6J (B6J). B6129SF1/J mice (Jackson Laboratory stock 101043), F1 offspring of a cross between B6J females and 129J males were used as wildtype controls (same SNP results as *Opn4*$^{-/-}$ mice). Additional *Opn4*$^{+/-}$ x *Opn4*$^{+/-}$ crosses were used to generate *Opn4*$^{+/+}$ littermate controls to confirm that the B6129SF1/J mice had similar refractive measurements (Figure S1). Therefore, we used B6129SF1/J mice as wildtype controls (referred to as *Opn4*$^{+/+}$) for the experiments using *Opn4*$^{-/-}$ and *Opn4*$^{DTA/DTA}$ mice.

In *Opn4*$^{DTA/DTA}$ mice, mRGCs are completely eliminated by introducing a gene encoding diphtheria toxin α subunit *(aDTA)* into the melanopsin gene locus (Guler et al., 2008). These mice lack both intrinsic and synaptic light input to mRGCs and show severe deficits in both PLR and circadian photoentrainment (Guler et al., 2008). SNP genome scanning analysis on *Opn4*$^{DTA/DTA}$ mice revealed similar genetic contribution from 129J and B6J as *Opn4*$^{-/-}$ mice, and hence B6129SF1/J mice were also used as wildtype controls for experiments involving these mice. An in-house breeding colony of male and female homozygous *Opn4*$^{-/-}$ and *Opn4*$^{DTA/DTA}$ mutant mice were maintained at the Atlanta Department of Veterans Affairs Health Care System. Mice were kept in 12:12 hour light/dark cycles (light phase: ~17 lux) with mouse chow and water accessible *ad libitum*.

2.2 Experimental design

Age-matched *Opn4*$^{+/+}$ and *Opn4*$^{-/-}$ mice were tested under two different experimental paradigms: normal refractive development and form-deprivation (FD). For normal refractive development experiments (*Opn4*$^{+/+}$, n=10; *Opn4*$^{-/-}$, n=12; *Opn4*$^{DTA/DTA}$, n=12 mice),

refractive error and ocular measurements were performed every two weeks from 4 to 16 weeks of age. For FD experiments, *Opn4*$^{+/+}$ mice (controls, n=8; FD, n=7 mice), *Opn4*$^{-/-}$ (controls, n=9; FD, n=12 mice), and *Opn4*$^{DTA/DTA}$ (controls, n=8; FD, n=8 mice) were fitted with a head-mounted diffuser goggle (Faulkner et al., 2007) over the right eye at 4 weeks of age, following baseline refractive error and ocular measurements. Weekly refractive measurements were performed on FD animals for 3 weeks (i.e. until 7 weeks of age). In some instances, weekly measurements were unable to be obtained for individual mice due to technical limitations and therefore, the sample sizes in the figure reflects the range of data points for each group.

Throughout the paper and figures we have compared between several different experimental groups of mice, defined below. ***Opn4***$^{+/+}$ (wildtype), ***Opn4***$^{-/-}$, and ***Opn4***$^{DTA/DTA}$ refer to the three different genotypes used in the study. **FD** refers to mice that were fitted with a diffuser goggle over the right eye so they received blurred visual input to that eye. **Opposite** refers to the non-FD eye (i.e. the contralateral eye that had intact visual input) from the same mice that were fitted with a diffuser goggle over the right eye. **Control** refers to a separate group of mice of any of the three genotypes that were not fitted with a diffuser goggle over the right eye, so they received intact visual input. Lastly, **naïve** refers to the combination of '**control**' group data from all three genotypes to compare to **FD** groups.

2.3 Refractive state, corneal curvature and ocular biometrics

Refractive error and ocular biometric measurements in mice were obtained, as described previously (Chakraborty et al., 2014; Pardue et al., 2008; Park et al., 2012; Park et al., 2014). After dilating the eyes with 1% tropicamide, refractive error in mice were first measured with an automated photorefractor by gently restraining the mouse by their tail in a dark room (Schaeffel et al., 2004). The animals were then anesthetized based on their body weight (ketamine 80 mg/kg; xylazine 16 mg/kg). A second set of more stable refractive measurements (standard deviation (SD) less than 0.5 diopters (D)) were taken under anesthesia (Pardue et al., 2008) and were used as the final measurements reported in the results. After refractive measurements, the anterior corneal radius of curvature was measured using an automated keratometer (repeatability within a SD of ± 0.02 mm) (Schaeffel, 2008; Schmucker and Schaeffel, 2004b).

Finally, biometric measurements of the mouse eye were taken with a 1310 nm spectral domain optical coherence tomography (SD-OCT) system (Bioptigen, Durham, NC, USA) (Chakraborty et al., 2014; Park et al., 2012). Ocular biometric parameters included: corneal thickness (CT), anterior chamber depth (ACD), lens thickness (LT), vitreous chamber depth (VCD), retinal thickness (RT), and axial length (AL). Axial length was measured by a masked observer from the anterior surface of the cornea to the anterior retinal pigment epithelium (RPE) border using the OCT calipers, calibrated with a refractive index of 1.43316 (Schmucker and Schaeffel, 2004a). During the experiments, the OCT system was upgraded to an Envisu R4300 SD-OCT (Bioptigen). Envisu SD-OCT has a better spatial resolution and lower intrasubject variability (0.004 ± 0.002 mm) (Bergen et al., 2016) for detecting the RPE border compared to the 1310 nm system (0.01 ± 0.01 mm) (Park et al., 2012). We found the instruments to have a consistent difference of 0.0411 mm and thus, the

1,310 nm OCT values were adjusted accordingly (Bergen et al., 2016). After the completion of all measurements, the mice were given yohimbine (2.1 mg/kg) to reverse the effects of anesthesia and to avoid the development of corneal lesions (Turner and Albassam, 2005). The mice were kept warm on a heating pad during recovery from anesthesia and saline eye drops were provided as needed.

2.4 Retinal dopamine (DA) quantification

To determine the levels of retinal DA and 3,4-Dihydroxyphenylacetic acid (DOPAC, the primary metabolic by-product of DA) (Witkovsky, 2004) during normal visual development in mice, the retinas were harvested between 10am and noon under controlled lighting conditions (fluorescent lighting, 600 lux) at different ages: 4 weeks of age (*Opn4*$^{+/+}$, n=10; *Opn4*$^{-/-}$, n=10; *Opn4*$^{DTA/DTA}$, n=10 mice), 8 weeks of age (*Opn4*$^{+/+}$, n=9; *Opn4*$^{-/-}$, n=11; *Opn4*$^{DTA/DTA}$, n=11 mice) and 12 weeks of age (*Opn4*$^{+/+}$, n=10; *Opn4*$^{-/-}$, n=6; *Opn4*$^{DTA/DTA}$, n=15 mice). For FD experiments, retinal DA and DOPAC levels were measured at 3 weeks of FD for *Opn4*$^{+/+}$ (control: n=7, FD: n=5 mice), *Opn4*$^{-/-}$ (control: n=5, FD, n=6 mice), and *Opn4*$^{+/+}$ mice (control: n=7, FD: n=3 mice). Experimental mouse retinas were collected 48 hours after the final measurements to minimize any residual effect of anesthesia, immediately frozen on dry ice, and stored at −80 °C. The frozen retinas were processed as previously described (Nir et al., 2000). Briefly, retinas were homogenized in a buffer solution containing 0.1 N $HClO_4$, 0.01% sodium metabisulfite and 50 ng/ml internal standard 3, 4-dihydroxybenzylamine and centrifuged. Supernatant fractions were separated with high-performance liquid chromatography (HPLC) using a mobile phase of 0.1 M sodium phosphate, 0.1 mM EDTA, 0.35 mM sodium octyl sulfate, and 6% acetonitrile (pH 3.0) to quantify the DA and DOPAC levels with coulometric detection. The DA and DOPAC levels were then calculated using a standard curve generated with 0.1–1 ng DA and DOPAC standard and normalized to aggregate protein concentration (ng/mg). For normal refractive development experiments, only retinas from the right eyes were used for analysis, while eyes of FD mice were analyzed individually. In addition, for both normal refractive development and FD experiments, a ratio of DOPAC by DA (DOPAC/DA ratio) was calculated as a measure of dopamine turnover.

2.5 Treatment with L-DOPA

We also examined the protective effects of dopamine treatment on spontaneous and FD-induced myopia in *Opn4*$^{-/-}$ mice. L-DOPA was administered from before birth by giving L-DOPA (1 mg/ml L-DOPA with 1 mg/ml ascorbic acid) *ad libitum* in drinking water to pregnant and nursing dams. After weaning at 3 weeks, pups continued to receive L-DOPA (1 mg/ml L-DOPA with 1 mg/ml ascorbic acid) through intraperitoneal daily injections (1 μl per gram body weight) until the end of the study. Solutions were freshly prepared 3 times a week and were protected from light. Control mice were not subjected to daily vehicle injections because vehicle injection had no significant effect on refractive error measurements or the response to form-deprivation in previous work (Landis et al., 2020; Mao et al., 2010). The effects of L-DOPA on refractive and ocular development of *Opn4*$^{-/-}$ mice were measured under both normal refractive development and FD visual paradigms. For normal refractive development experiments, refractive measurements were obtained at 4 and 6 weeks of age to study protective effects of dopamine against naturally occurring

myopia in juvenile *Opn4*$^{-/-}$ animals (n=6). For the FD paradigm, baseline refractive and ocular measurements were taken on a group of *Opn4*$^{-/-}$ mice (naïve controls, n=5; FD, n=7 mice) at 4 weeks of age. Mice were then form-deprived for 2 weeks and were measured weekly. Finally, retinas from both non-FD and FD experiments were harvested at 6 weeks of age (as described earlier) for examining the changes in retinal DA and DOPAC levels with L-DOPA treatment.

2.6 Data analysis

Two-way repeated-measures mixed-effects analysis (fully abbreviated as 'MEA'), or ANOVA where applicable, with Holm-Sidak multiple comparisons (fully abbreviated as 'HSK') (GraphPad Prism, San Diego, CA) was performed to examine the differences between the *Opn4*$^{+/+}$ and *Opn4*$^{-/-}$ (or *Opn4*$^{DTA/DTA}$) animals and between control animals and those treated with L-DOPA with intact and FD visual conditions, across age. Given the similar genetic composition of *Opn4*$^{-/-}$ and *Opn4*$^{DTA/DTA}$ animals, the same cohort of B6129SF1/J wildtype mice was used for comparison against both mouse genotypes. All the results are reported as an interaction effect unless stated otherwise. For normal refractive development experiments, refractive and biometric measurements from the two eyes were averaged as both eyes received the same treatment. If a measurement could not be obtained on a single eye on a particular day due to technical considerations, then the available single eye measurement was used. For FD experiments, the effect of FD on refraction was calculated as a "shift" (i.e. the difference in the measured value between the FD (right, OD) and contralateral (left, OS) eyes). To eliminate any inter-subject variability, the axial length, corneal radii, and other ocular measurements of the FD cohorts were normalized to their 4-week-old baseline values (by dividing by the 4-week-old baseline) before calculating "shifts". For normal refractive development cohorts, the differences in DA and DOPAC values between the two genotypes across different ages were calculated using a MEA, or ANOVA where applicable, with HSK. A one-way ANOVA with HSK was used to analyze the DA data from FD experiments. Changes in retinal DA parameters between the L-DOPA and controls were analyzed with Welch's t-test. DA L-DOPA experiment parameters with FD were analyzed with one-way ANOVA with HSK. Cell counts were analyzed using one-way ANOVA with HSK. All data are expressed as mean ± standard error of mean (SEM) with significance labeled in the figure legends.

3. Results

3.1 Abnormal refractive development and axial eye growth in mRGC mutant mice

In this study, we measured refractive and ocular development, as well as dopaminergic activity, in mice that had either a null mutation in the *Opn4* gene encoding melanopsin (*Opn4*$^{-/-}$) or genetically ablated mRGCs (*Opn4*$^{DTA/DTA}$). With intact visual input, *Opn4*$^{-/-}$ mice were significantly more myopic at younger ages than *Opn4*$^{+/+}$ mice (refractive error at 4 weeks, −3.56 ± 0.35 vs +0.73 ± 0.51 diopters (D), MEA with HSK, $p<0.001$, Figure 1A). Additionally, the refractions of *Opn4*$^{-/-}$ mice shifted towards hyperopia at a 3 times greater rate than wild-type mice (*Opn4*$^{-/-}$, 0.9 D / week, $R^2 = 0.90$; *Opn4*$^{+/+}$, 0.3 D / week, $R^2 = 0.92$; linear regression analysis, $p<0.001$) leading to an overall difference in refractive development (MEA; age by genotype interaction, $F(6,117) = 25.40$, $p<0.001$). As a result,

adult *Opn4*$^{-/-}$ mice tended to be hyperopic relative to *Opn4*$^{+/+}$ mice at 16 weeks (+6.53 ± 0.33 vs +4.52 ± 0.88 D).

To compare the absence of melanopsin to the lack of mRGCs on ocular growth in rodents we also compared refractive development in *Opn4*$^{DTA/DTA}$ mice to the other genotypes. When visual input was intact, the absence of mRGCs led to significant differences in the refractive development of *Opn4*$^{DTA/DTA}$ mice compared to both *Opn4*$^{+/+}$ and *Opn4*$^{-/-}$ mice (MEA; age by genotype interaction, $F(12,179) = 15.10$, $p<0.001$, Figure 1A). Both *Opn4*$^{+/+}$ and *Opn4*$^{DTA/DTA}$ mice started with similar, near emmetropic refractive errors at 4 weeks. However, starting from 6 weeks, *Opn4*$^{DTA/DTA}$ animals showed a significantly greater shift toward hyperopic refractions, with a rate of ~0.5 D / week (R^2=0.70, linear regression analysis, p=0.009; average change in refraction after 10 weeks: +7.42 ± 0.58 D), than their *Opn4*$^{+/+}$ counterparts (0.3 D / week, $R^2 = 0.90$; +2.92 ± 0.82 D; HSK at all ages starting from 6 weeks, $p<0.05$). In comparison with *Opn4*$^{-/-}$ mice, *Opn4*$^{DTA/DTA}$ mice on average were ~3 – 4 D more hyperopic at all but the oldest ages (mean refraction at 10 weeks: *Opn4*$^{-/-}$, +3.98 ± 0.36 D; *Opn4*$^{DTA/DTA}$, +7.72 ± 0.34 D, HSK at 4–12 weeks: $p<0.001$, 14 weeks: $p<0.01$, 16 weeks: $p<0.05$). Therefore, both *Opn4*$^{-/-}$ (0.9 D / week) and *Opn4*$^{DTA/DTA}$ mice have steeper refractive development curves compared to *Opn4*$^{+/+}$ mice. These data suggest that the absence of mRGC signaling accelerates the shift toward hyperopic refraction in mice.

Consistent with greater hyperopic refractions in older ages, *Opn4*$^{-/-}$ mice exhibited significantly shorter axial lengths than wild-type mice from 10 to 16 weeks (16 weeks: *Opn4*$^{+/+}$, 3.42 ± 0.01 mm; *Opn4*$^{-/-}$, 3.34 ± 0.01 mm, MEA; age by genotype interaction, $F(6,87) = 8.935$, $p<0.001$, Figure 1B). Likewise, *Opn4*$^{DTA/DTA}$ mice had significantly shorter axial lengths at all measurement ages compared with *Opn4*$^{+/+}$ mice (MEA; main effect of genotype, $F(6,86) = 10.12$, $p<0.001$). Axial lengths of adult *Opn4*$^{DTA/DTA}$ animals were also significantly shorter than *Opn4*$^{-/-}$ mice (mean at 10 weeks: *Opn4*$^{-/-}$, 3.26 ± 0.01 mm; *Opn4*$^{DTA/DTA}$, 3.22 ± 0.01 mm, HSK at weeks 4, 10, 12, and 16, $p<0.05$).

Corneal curvature between *Opn4*$^{+/+}$ and *Opn4*$^{-/-}$ mice was not significantly different (MEA), however both showed significant corneal flattening with age (change in corneal radii from 4–14 weeks: *Opn4*$^{+/+}$, 0.19 ± 0.01 mm; *Opn4*$^{-/-}$, 0.16 ± 0.01 mm, MEA; main effect of age, $F(3.1,60.3) = 500.2$, $p<0.001$, Figure 1C). Similarly, *Opn4*$^{DTA/DTA}$ mice exhibited a significant age-related flattening of the cornea throughout development (total change in corneal radii across development: *Opn4*$^{+/+}$, 0.20 ± 0.01; *Opn4*$^{-/-}$, 0.18 ± 0.01; *Opn4*$^{DTA/DTA}$, 0.18 ± 0.01 mm, MEA; main effect of age, $F(3.8,115.4) = 594.4$, $p<0.001$) but was not different than the other two groups (MEA; main effect of genotype, $F(2, 31) = 0.02$, p=0.98).

Opn4$^{-/-}$ mice also had significant changes in other ocular parameters, some of which could contribute to the altered refractive development and hyperopic refractions (Table S1). Among these, anterior chamber depth (ACD) was shorter (average across all ages: *Opn4*$^{+/+}$, 0.37 ± 0.004 mm; *Opn4*$^{-/-}$, 0.35 ± 0.002 mm, MEA; main effect of genotype, $F(1,18) = 25.18$, $p<0.001$, Figure S2A) and vitreous chamber depth (VCD) was longer (MEA; main effect of genotype, $F(1,18) = 5.86$, p=0.026, Figure S2B). However, since there was no

change in the crystalline lens thickness between *Opn4*$^{+/+}$ and *Opn4*$^{-/-}$ mice (LT, Figure S2C), our results suggest a slight anterior displacement of the lens of *Opn4*$^{-/-}$ mice causing myopic refractions in younger mice, and a gradual reduction in axial length with age causing hyperopic refractions in older mice (Figure S2D–E). Likewise, *Opn4*$^{DTA/DTA}$ mice had significantly shallower ACD (mean length across all ages, 0.327 ± 0.003 mm, MEA; main effect of genotype), suggesting a similar lens displacement as in *Opn4*$^{-/-}$ mice (0.35 ± 0.002 mm). *Opn4*$^{DTA/DTA}$ mice also had thinner retinas (mean thickness across all ages; 0.195 ± 0.003 mm) compared to both *Opn4*$^{+/+}$ (0.232 ± 0.002 mm, $p<0.001$) and *Opn4*$^{-/-}$ mice (0.220 ± 0.002 mm, $p<0.001$, MEA; main effect of genotype, Table S2). *Opn4*$^{DTA/DTA}$ mice were not different in VCD, LT, or CT (MEA; main effect of genotype, all $p>0.05$).

3.2 Enhanced susceptibility to FD myopia with the loss of melanopsin signaling

Since we found significant differences in refractive development between *Opn4*$^{+/+}$, *Opn4*$^{-/-}$, and *Opn4*$^{DTA/DTA}$ mice, we next investigated if these differences translated into different responses to FD myopia. *Opn4*$^{+/+}$ mice developed FD myopia after 3 weeks of goggle wear, leading to a significantly greater myopic shift (difference between the FD eye, fitted with a diffuser goggle, and the opposite contralateral eye, not fitted with a diffuser goggle, see Methods). Importantly, non-FD, control mice that were not fitted with a diffuser goggle over either eye, developed no myopic shift between eyes and the refractive difference remained close to 0 D. FD *Opn4*$^{+/+}$ mice became myopic (ANOVA; age by treatment interaction, $F(3,36) = 3.13$, $p=0.037$) and had ~1 D of myopic shift compared to controls after 3 weeks of FD (−1.11 ± 0.31 vs +0.14 ± 0.28 D, HSK, $p=0.047$, Figure 2A). However, there was no change in axial length (Figure 2B) or corneal curvature shifts (Figure 2C) normalized to their 4-week baseline. After 3 weeks of FD, *Opn4*$^{-/-}$ FD mice, however, had almost 4 times greater myopic refractive shift than control mice (−3.52 ± 0.52 vs +0.23 ± 0.36 D, MEA; age by treatment interaction, $F(3,53) = 9.57$, $p<0.001$, Figure 2D). As with *Opn4*$^{+/+}$ mice, FD in *Opn4*$^{-/-}$ mice did not significantly affect axial length shifts (Figure 2E). Yet, *Opn4*$^{-/-}$ mice did develop significantly steeper corneal curvatures with FD compared to controls (after 3 weeks of FD: FD, −0.02 ± 0.01 mm; control, +0.01 ± 0.01 mm, MEA; main effect of treatment, $F(1,14) = 6.22$, $p=0.026$, Figure 2F). Lastly, the differences between control and FD *Opn4*$^{DTA/DTA}$ mice closely resembled those of *Opn4*$^{-/-}$ mice. FD caused a large myopic shift in *Opn4*$^{DTA/DTA}$ mice after 3 weeks (−3.16 ± 1.09 vs +0.10 ± 0.40 D, MEA; main effect of treatment $p=0.004$, Figure 2G). There were no major differences between FD and control *Opn4*$^{DTA/DTA}$ mice in axial length (Figure 2H) or corneal curvature (Figure 2I). Additionally, FD did not cause significant changes in any other ocular biometric parameter for any genotype (Table S3).

To compare across mice, the refractive shift in the control animals from all three genotypes were averaged together as one group, since there was no difference between them (naïve group, n=25, MEA; main effect of genotype, $F(2,22) = 0.1384$, $p=0.87$, see Methods). Compared to naïve animals (mean refractive shift after 3 weeks, 0.16 ± 0.20 D), FD mice from all three groups developed significant myopia after 3 weeks of FD (MEA; age by genotype interaction, $F(9,132) = 4.60$, $p<0.001$, Figure 2J). *Opn4*$^{-/-}$ mice had significantly greater myopic shifts compared to *Opn4*$^{+/+}$ mice (MEA; main effect of genotype, $F(1,16) = 7.79$, $p=0.013$). This difference was a result of ~3 times greater rate of myopia development

in *Opn4*$^{-/-}$ mice (*Opn4*$^{+/+}$, −0.34 D / week, R^2 = −0.98; *Opn4*$^{-/-}$, −0.96 D / week, R^2 = 0.99; linear regression analysis, p<0.001). Furthermore, *Opn4*$^{DTA/DTA}$ mice developed myopia at a similar rate as *Opn4*$^{-/-}$ mice (−0.96 vs −1.03 D / week, linear regression analysis, p=0.55) and were not significantly different than *Opn4*$^{-/-}$ mice (MEA; main effect of genotype, F (1,18) = 0.97, p=0.34). The myopic shift in FD *Opn4*$^{DTA/DTA}$ mice was on average larger than naïve and FD *Opn4*$^{+/+}$ mice by ~3 D at 3 weeks post-FD (MEA; age by genotype interaction, F (9,132) = 4.60, p<0.001). Three weeks of FD did not cause significant changes in axial length compared across genotype (MEA with HSK, main effect of genotype, F (3,41) = 1.09, p=0.36, Figure 2K). However, *Opn4*$^{DTA/DTA}$ mice had steeper corneal radii after FD when directly compared to *Opn4*$^{+/+}$ mice after FD (MEA, main effect of genotype, F (1,9) = 7.16, p<0.05) but there were no other differences between groups (Figure 2L). Lastly, there were no differences between genotypes of any other ocular parameter (Table S4).

3.3 Absence of melanopsin alters retinal dopamine (DA) and DOPAC levels in normal and FD mice

Under intact visual conditions, DOPAC levels were similar between *Opn4*$^{+/+}$ and *Opn4*$^{-/-}$ retinas (MEA; main effect of genotype, F (1,20) = 0.161, p=0.69, Figure 3A). However, mRGC absence significantly elevated DOPAC levels in the retinas of 4-week old *Opn4*$^{DTA/DTA}$ mice (0.63 ± 0.03 ng/mg retina vs 0.30 ± 0.03 and 0.26 ± 0.01 ng/mg retina in *Opn4*$^{+/+}$ and *Opn4*$^{-/-}$ respectively), but not 8 and 12 week-old mice (MEA; age by genotype interaction, F (4,49) = 8.143, p<0.001). Furthermore, DA levels were significantly higher in *Opn4*$^{DTA/DTA}$ retinas compared to *Opn4*$^{+/+}$ and *Opn4*$^{-/-}$ retinas at 8 (1.50 ± 0.04 vs 1.18 ± 0.06 and 1.17 ± 0.04 ng/mg, respectively, HSK) and 12 (1.64 ± 0.06 vs 1.38 ± 0.05 and 1.22 ± 0.07 ng/mg retina, respectively, HSK) weeks of age (MEA; age by genotype interaction, F (4,83) = 2.52, p=0.05, Figure 3B). However, there were no significant differences between *Opn4*$^{-/-}$ and *Opn4*$^{+/+}$ mice across all ages (HSK). The DOPAC/DA ratio did not change between *Opn4*$^{+/+}$ and *Opn4*$^{-/-}$ genotypes (MEA; main effect of genotype, F (1,20) = 0.297, p=0.59, Figure 3C). However, the DOPAC/DA ratio in young *Opn4*$^{DTA/DTA}$ mice was significantly greater (average at 4 weeks: 0.40 ± 0.03 ng/mg retina) than both *Opn4*$^{+/+}$ (0.19 ± 0.03) and *Opn4*$^{-/-}$ mice (0.19 ± 0.01) (MEA; age by genotype interaction, F (4,83) = 8.98, p<0.001). In addition to changes between genotypes, age also affected retinal DA and DOPAC levels. Both DOPAC and the DOPAC/DA ratio significantly increased after 4 weeks of age in *Opn4*$^{+/+}$ and *Opn4*$^{-/-}$ mice while they decreased in *Opn4*$^{DTA/DTA}$ mice (MEA; age by genotype interaction: DOPAC: F (4,49) = 8.143, p<0.001; DOPAC/DA: F (4,83) = 8.975, p<0.001).

After 3 weeks of FD, *Opn4*$^{+/+}$ mice showed no significant differences in retinal DOPAC, DA, or DOPAC/DA ratios between different treatment groups (one-way ANOVA, all p>0.05, Figure 3D–F). In contrast, FD *Opn4*$^{-/-}$ retinas had significantly lower DOPAC levels (0.21 ± 0.01 ng/mg retina) than opposite (0.30 ± 0.02 ng/mg retina) retinas (one-way ANOVA F (2,12) = 5.20, p= 0.023; Figure 3G). FD *Opn4*$^{-/-}$ retinas also had on average lower DA levels (1.06 ± 0.02 ng/mg) compared to opposite (1.28 ± 0.08 ng/mg) retinas (one-way ANOVA F (2,12) = 2.89, p=0.094; Figure 3H). However, DOPAC/DA ratios were similar between the three groups (one-way ANOVA, F (2,12) = 1.59, p=0.244, Figure 3I). Finally,

there were no differences between *Opn4*$^{DTA/DTA}$ control and FD eyes in DOPAC, DA, or the DOPAC/DA ratio (one way ANOVA genotype interactions: F (2,10) = 0.32, p=0.74, F (2,10) = 2.13 p=0.17, and F (2,10) = 0.11, p=0.89, respectively, Figure 3J–L).

3.4 L-DOPA treatment prevents FD myopia but not spontaneous myopia in young Opn4$^{-/-}$ mice

We found that *Opn4*$^{-/-}$ mice had reduced levels of DOPAC, and likely DA (Figure 3), in FD eyes suggesting a deficiency related to melanopsin-mediated mRGC signaling. Interestingly, when mRGCs were ablated, there was no change in DOPAC or DA levels in FD eyes, despite elevated levels in normal refractive development. Therefore, we examined the protective effects of chronic L-DOPA treatment on myopic refraction only in *Opn4*$^{-/-}$ mice to determine whether supplementation could attenuate refractive and ocular changes with FD. L-DOPA treatment started before birth did not prevent spontaneous myopia in 4 and 6 week-old juvenile *Opn4*$^{-/-}$ mice (at 6 weeks: *Opn4*$^{-/-}$, −1.78 ± 0.40 D; +L-DOPA, −1.80 ± 0.65 D, MEA; main effect of treatment, F (1,16) = 0.095, p=0.76; main effect of age, F(1,14) = 66.18, p<0.001, Figure 4A). With intact vision, L-DOPA treatment did not cause significant changes between groups in axial length (MEA, p=0.48, Figure 4B) or almost all other ocular parameters (data not shown). However, L-DOPA treated *Opn4*$^{-/-}$ mice showed a significant steepening of the corneal radii compared to un-treated *Opn4*$^{-/-}$ mice (mean across 4 and 6 weeks: *Opn4*$^{-/-}$ vs +L-DOPA, 1.40 ± 0.01 vs 1.37 ± 0.004 mm, ANOVA; main effect of treatment, F (1,16) =22.47, p<0.001, Figure 4C). L-DOPA treatment started before birth and FD started at 4 weeks of age caused a significant reduction of FD myopia in *Opn4*$^{-/-}$ mice compared to control animals (MEA; age by treatment interaction, F (4,55) = 3.50, p=0.013, Figure 4D). Since there were no significant differences in refraction of *Opn4*$^{-/-}$ naïve control animals and L-DOPA treated control groups (MEA, p=0.82), they were averaged together as the “control” group for this analysis. Compared to control animals (0.12 ± 0.25 D), 2 weeks of FD produced a significant myopic shift of −2.74 ± 0.54 D in *Opn4*$^{-/-}$ mice (HSK after two weeks of FD, p<0.001; Figure 4D). Although L-DOPA treated FD *Opn4*$^{-/-}$ animals exhibited a myopic shift (−1.34 ± 0.41 D), it was half the magnitude seen in *Opn4*$^{-/-}$ mice that did not receive L-DOPA (HSK, p=0.055) due to slower development (−0.42 vs −1.02 D / week, linear regression). L-DOPA treatment did not lead to significant changes in axial length or corneal radii of FD animals (MEA, p>0.05, Figure 4E–F).

Six week-old L-DOPA treated eyes had significantly elevated levels of retinal DOPAC (0.46 ± 0.03 ng/mg retina) and DA (1.67 ± 0.15 ng/mg retina) compared to non-treated *Opn4*$^{-/-}$ eyes (DOPAC, 0.31 ± 0.02, p=0.002; DA, 1.27 ± 0.03 ng/mg retina, p=0.044, Welch’s t-tests, Figure S3A–B). However, this increase did not alter the myopic refractive error compared to non-L-DOPA treated mice, suggesting that DA may not be associated with the myopic phenotype seen in young *Opn4*$^{-/-}$ animals. DA turnover (DOPAC/DA ratio) did not differ with L-DOPA treatment (L-DOPA treated, 0.28 ± 0.02 ng/mg retina; control, 0.25 ± 0.01 ng/mg retina, Welch’s t-test, p=0.22, Figure S3C). Consistent with inhibitory effects of DA on FD myopia, L-DOPA treated *Opn4*$^{-/-}$ animals showed no difference in DA or DOPAC levels between FD and opposite or control eyes, (all one-way ANOVA comparisons, p>0.05, Figure S3D–F) unlike non-L-DOPA treated *Opn4*$^{-/-}$ mice (Figure

3G–H). Furthermore, DOPAC and DA were significantly higher in L-DOPA treated FD eyes than non-treated FD eyes (DOPAC, 0.35 ± 0.09 vs 0.21 ± 0.02 ng/mg retina, p=0.004; DA, 1.51 ± 0.22 vs 1.02 ± 0.04 ng/mg retina, p=0.001; Welch's t-tests). Overall, these findings suggest that DA insufficiency in melanopsin deficient retinas at least partly underlies high susceptibility to FD myopia in *Opn4*$^{-/-}$ mice.

4. Discussion

mRGCs are environmental irradiance detectors that project to the brain centers controlling circadian rhythms and pupil size (Berson et al., 2002; Hattar et al., 2002; Panda et al., 2002). These cells also regulate endogenous retinal circadian rhythms through their intrinsic photoreception and by modulating the diurnal activity of DA in the retina (Storch et al., 2007; Tosini et al., 2008). Using two mutant mouse models, we found that signaling through mRGC pathways is critical for normal pre-natal and post-natal refractive development, for regulating the response to FD, and for maintaining correct dopaminergic signaling (Figure 5A). In the first set of experiments, the absence of the melanopsin photopigments and intrinsic melanopsin light responses of mRGCs in *Opn4*$^{-/-}$ mice resulted in abnormal refractive development and greater susceptibility to FD myopia (Figure 5B). The increased susceptibility to myopia in *Opn4*$^{-/-}$ mice was found to be associated with lower dopaminergic activity in the retina and was partly attenuated with L-DOPA treatment. In the second set of experiments, we found that a complete loss of mRGCs led to significantly more hyperopic refractions in *Opn4*$^{DTA/DTA}$ mice than *Opn4*$^{-/-}$ mice, but a similar myopic response to FD compared to *Opn4*$^{-/-}$ mice. Overall, these results show strong and complex interactions between mRGCs and refractive control in mouse eyes.

4.1 Intact retinal melanopsin pathways are critical for normal refractive development

With intact vision, 4 and 6 week-old *Opn4*$^{-/-}$ mice were ~4 – 5 D more myopic than *Opn4*$^{+/+}$ mice, but then became significantly more hyperopic than their *Opn4*$^{+/+}$ counterparts at older ages (Figure 1). The pattern of refractive development in *Opn4*$^{-/-}$ mice could be explained by ocular biometric changes in these eyes. At the youngest ages, *Opn4*$^{-/-}$ mice on average had significantly shallower anterior chamber and longer vitreous chamber than *Opn4*$^{+/+}$ mice, without any significant differences in the crystalline lens thickness between the two genotypes (Figure S2, Table S1). This suggests a slight anterior positioning of the lens in *Opn4*$^{-/-}$ mice compared to *Opn4*$^{+/+}$ animals. With the axial length similar to *Opn4*$^{+/+}$ mice at 4 and 6 weeks, the positioning of the lens away from the retina would induce a myopic refractive error in *Opn4*$^{-/-}$ mice due to the change in the eye's effective power (Collins et al., 1995; Erickson, 1990). In older mice between 8 and 16 weeks of age, the hyperopic refractions are likely caused by reduced lengthening of the axial length with age in *Opn4*$^{-/-}$ vs. *Opn4*$^{+/+}$ mice, a response that may counteract the refractive shift produced by the displacement of the lens.

When mRGCs are ablated in *Opn4*$^{DTA/DTA}$ mice and their refractive development is compared to *Opn4*$^{-/-}$, we can determine the contribution of intrinsic mRGC signaling via rod/cone photoreceptor pathways to refractive development (Figure 1) independent of melanopsin activity. We confirmed our hypothesis that *Opn4*$^{DTA/DTA}$ mice would

have a more severe refractive phenotype: *Opn4*$^{DTA/DTA}$ mice were significantly more hyperopic across development than *Opn4*$^{-/-}$ as well as *Opn4*$^{+/+}$ mice. While absence of intrinsic signaling from otherwise intact mRGCs contributes more to the rate of refractive development, photoreceptor-mediated synaptic input appears to influence the end-point and rate of refractive change. As wildtype refractive development reaches the typical +3 −4 D refractive error at 12 weeks, the lack of mRGC signaling recalibrates the setpoint of refractive development and accelerates attaining the target refraction to just 6 weeks. The differences in refractive development between *Opn4*$^{-/-}$ and *Opn4*$^{DTA/DTA}$ might be related to different mRGC subtypes, such as M1 that are primarily intrinsic photoreceptors whereas M2 and M3 primarily receive their input from rods and cones (Schmidt and Kofuji, 2011). Additionally, both *Opn4*$^{-/-}$ and *Opn4*$^{DTA/DTA}$ had shorter axial lengths with reduced anterior chamber depths and thinner retinas (Figures 1 and S2, Tables S1 and S2), resulting in hyperopia in eyes with intact visual input. Overall, these results suggest that signaling from mRGCs plays an important role in normal refractive development of the eye.

4.2 Altered mRGC signaling impacts FD myopia in mice

We found that both *Opn4*$^{-/-}$ and *Opn4*$^{+/+}$ mice developed significant myopia after 3 weeks of FD. However, the magnitude of the myopic shift in *Opn4*$^{-/-}$ mice was 3 times larger than the myopic shift in *Opn4*$^{+/+}$ animals (Figure 2). Interestingly, *Opn4*$^{DTA/DTA}$ mice had a comparable myopic shift to *Opn4*$^{-/-}$ mice suggesting that ablating mRGCs exerts the same effect on myopia progression as removing melanopsin from these cells. Mirroring the large difference in myopic shifts between genotypes, myopia development of *Opn4*$^{DTA/DTA}$ (and *Opn4*$^{-/-}$) mice progressed significantly faster than naïve and *Opn4*$^{+/+}$ FD mice (*Opn4*$^{DTA/DTA}$ vs *Opn4*$^{-/-}$ vs *Opn4*$^{+/+}$ vs naïve: −1.03 vs −0.96 vs −0.34 vs 0.11 D / week, linear regression analysis, $p<0.001$). These results indicate that intact mRGC signaling slows the development of FD myopia. Previously, molecular analyses of the chick retina following 6 hours of experimentally induced myopia or hyperopia identified differentially expressed intrinsic circadian clock genes, including the melanopsin gene (Stone et al., 2011b; Stone et al., 2020). In another recent study, retinal-specific knockout of the clock gene *Bmal1* induced myopia in mice, whereas knockouts of clock genes *cycle or period* induced elongation of the pseudocones (the optical component that separates the facet lens from the photoreceptors in the fly eye) in *Drosophila melanogaster*, suggesting that the effects of circadian disruption on ocular development and myopia can be seen in widely separated species (Stone et al., 2019). The present results reinforce a potential association between retinal circadian clocks, refractive development, and myopia (Chakraborty et al., 2018) by highlighting a role for mRGCs.

The myopic shifts in form-deprived *Opn4*$^{-/-}$ mice were not associated with changes in any of the ocular biometric parameters, including axial length. Melanopsin deficient *Opn4*$^{-/-}$ mice also showed a significant steepening of the cornea with FD. Previous studies have found melanopsin expression in corneal sensory nerves, and a potential role of melanopsin in corneal function (Delwig et al., 2018; Matynia et al., 2015) might be involved in mediating these corneal changes with FD. Furthermore, it may be that environments associated with myopia progression (e.g. blurred, defocused, or indoor conditions) (Flitcroft et al., 2020; Lingham et al., 2020), which contain lower spatial frequency information

similar to FD, reduce signaling of mRGCs and increase the susceptibility to FD myopia in *Opn4*$^{-/-}$ mice (Figure 2). Together, these results suggest that mRGCs are important for modulating the susceptibility to FD myopia in mice, but this susceptibility does not depend on intrinsic versus synaptic mRGC signaling.

4.3 Altered dopaminergic activity underlies increased susceptibility to FD in Opn4$^{+/+}$, but not abnormal refractive development in Opn4$^{-/-}$ mice

In the absence of melanopsin, *Opn4*$^{-/-}$ mice experiencing normal vision did not have lower retinal DA across all ages (Figure 3b). While it has been demonstrated that mRGC signaling can alter retinal dopaminergic signals (Zhang et al., 2012; Zhang et al., 2008), notably however, a study by Cameron et al. found that melanopsin is neither necessary nor sufficient for light-regulated release of retinal DA (Cameron et al., 2009). Importantly, *Opn4*$^{-/-}$ mice had similar DOPAC levels and DOPAC/DA ratios as *Opn4*$^{+/+}$ mice across all ages, indicating that reduced input to mRCGs does not necessarily alter DA metabolism, signaling, and turnover in *Opn4*$^{-/-}$ retinas (Figure 3). However, since *Opn4*$^{DTA/DTA}$ mice had increased DA and DOPAC levels, and thus increased DA turnover, especially at young ages, our data suggest that the complete absence of mRGCs, and potentially less drive to dopaminergic amacrine cells, causes significant dysregulation of the dopaminergic system and may explain their hyperopic refractions and shorter axial lengths. Unlike in *Opn4*$^{-/-}$ mice, DA appears to play an important role in regulation of normal refractive development in *Opn4*$^{DTA/DTA}$ mice. Therefore, synaptic input to mRGCs through photoreceptor pathways in *Opn4*$^{-/-}$ mice is likely sufficient for normal DA metabolism and turnover. Given that endogenous levels of retinal DOPAC and the DOPAC/DA ratio are more important than DA levels for determining the myopia susceptibility in the mouse eye (Chakraborty and Pardue, 2015; Chakraborty et al., 2014; Chakraborty et al., 2015), these findings suggest that juvenile myopia and abnormal refractive development in mice lacking melanopsin (*Opn4*$^{-/-}$) are independent of dopaminergic mechanisms, but that photoreceptor input is necessary. This is further supported by the fact that chronic treatment with L-DOPA from before birth could not prevent spontaneous myopia in young 4 and 6 week-old *Opn4*$^{-/-}$ mice, despite elevated levels of retinal DOPAC and DA with the treatment (Figure 4, Figure S3). Interestingly, L-DOPA treated *Opn4*$^{-/-}$ mice showed steepening of the cornea in comparison with non-treated mice, which could be a result of changes in the corneal dopamine receptor activity with DA treatment (Cavallotti et al., 1999; Crosson et al., 1984).

As shown in Figure 3, *Opn4*$^{-/-}$ mice that developed significant myopia with FD also had significantly lower levels of retinal DOPAC (and DA although statistically insignificant) in their FD eyes, suggesting an important role of DA metabolism in FD in these mice. This was consistent with previous reports of lower DOPAC and DA levels in chicken (Stone et al., 1989) and primate (Iuvone et al., 1989) eyes with FD myopia. In contrast, DA is unlikely to play a role in FD myopia in *Opn4*$^{DTA/DTA}$ mice, due to a lack of DA differences, suggesting that DA regulation of FD myopia requires intact photoreceptor signals through mRGCs. Furthermore, systemic administration of L-DOPA has been shown to prevent the development of FD myopia in mammalian eyes (Landis et al., 2020; Mao et al., 2010) and L-DOPA supplementation in FD *Opn4*$^{-/-}$ mice reduced the myopic shift magnitude to almost half compared to FD mice that did not receive the treatment (p=0.055, Figure 4).

This is consistent with evidence of dopamine acting as a "stop signal" for experimental myopia in animals (Dong et al., 2011; Iuvone et al., 1989; Stone et al., 1989). Additionally, the protective effects of L-DOPA treatment in myopic *Opn4*$^{-/-}$ eyes were associated with elevated levels of retinal DOPAC and DA when compared to non-treated *Opn4*$^{-/-}$ eyes (Figures 4 and S2). This supports previous work showing that systemic L-DOPA treatment can pass the blood-retinal barrier to accumulate in the retina as well as increase levels of retinal DA and DOPAC (Chesler et al., 2021; Mao et al., 2010). Note that we only tested the effects of a single L-DOPA concentration (1 mg/mL) on FD myopia, which may not have been sufficient to elicit complete suppression of myopia or affect DA and DOPAC levels during FD. Therefore, future studies examining the efficacy of higher doses of L-DOPA on FD myopia in *Opn4*$^{-/-}$ mice are warranted because L-DOPA inhibited the development of experimental myopia in a dose-dependent manner in chickens (Thomson et al., 2019; Thomson et al., 2020). Interestingly, while FD and L-DOPA treatments individually caused corneal steeping in *Opn4*$^{-/-}$ mice, FD treated with L-DOPA did not affect corneal curvature (Figure 4), suggesting complex interactions between corneal melanopsin and DA receptors under different visual conditions.

4.5 Conclusions: mRGCs impact refractive development and myopia progression in mice

The prevalence of myopia worldwide is increasing at an alarming rate, especially in some regions of Asia (Dolgin, 2015; Wu et al., 2016), and affects around 30% of the population globally (Holden et al., 2016; Morgan et al., 2017). Importantly, as myopia increases, so do the rates of many blinding conditions in adulthood (Morgan et al., 2012). However, the underlying mechanisms responsible for myopia are unknown and novel mechanistic approaches are needed to identify more effective preventative and therapeutic methods. Our results add to the growing evidence of a potential underlying link between melanopsin, circadian rhythms, visual signaling, and the hypothesis of circadian dysregulation as a mechanism for myopia development (Chakraborty et al., 2020; Chakraborty et al., 2018; Stone et al., 2013). Melanopsin signaling has been the target of intense research in the past decade and plays a role in many important visual functions. We found that melanopsin signaling has pronounced effects on both normal refractive development and the eye's response to FD, a widely studied myopia model in experimental animals. Additionally, we have found that these changes are associated with changes in axial length and other ocular parameters in the mouse eye. Lastly, our work adds further support to the widely-reported involvement of the retinal dopamine system in myopia by providing evidence to link of dopaminergic activity with mRGCs. Taken together, we conclude that proper mRGC function can protect against myopia and myopia progression and suggest that mRGC function could be a potential target for myopia intervention.

Supplementary Material

Refer to Web version on PubMed Central for supplementary material.

Funding:

This project was supported by the National Institutes of Health [NIH R01 EY016435 (MTP), NIH R01 EY004864 and NIH R01 EY027711 (PMI), NIH R01 EY022342 (RAS), NIH P30 EY006360, T32 EY007092 (EGL)],

Department of Veterans Affairs [Rehabilitation R&D Service Research Career Scientist Award IK6 RX003134 (MTP)], and Research to Prevent Blindness [Departmental Award]. The funding organizations had no role in the design or conducting of this research.

Disclaimer: E.G. Landis is currently employed by the National Institutes of Health which funded this study, but this study was performed prior to her work at NIH. The opinions statements contained in this manuscript do not represent the views of the NIH or the Department of Health and Human Services.

Abbreviations:

mRGC	melanopsin-expressing retinal ganglion cell
DA	dopamine
DOPAC	L-3,4-dihydroxyphenylalanine
FD	form-deprivation
L-DOPA	L-3,4-dihydroxyphenylalanine
CT	corneal thickness
ACD	anterior chamber depth
LT	lens thickness
VCD	vitreous chamber depth
RT	retinal thickness
AL	axial length
CC	corneal curvature
MEA	two-way repeated-measures mixed-effects analysis
HSK	Holm-Sidak multiple comparisons posthoc test

References

Ashby R, McCarthy CS, Maleszka R, Megaw P, Morgan IG, 2007. A muscarinic cholinergic antagonist and a dopamine agonist rapidly increase ZENK mRNA expression in the form-deprived chicken retina. Experimental eye research 85, 15–22. [PubMed: 17498696]

Bergen MA, Park HN, Chakraborty R, Landis EG, Sidhu C, He L, Iuvone PM, Pardue MT, 2016. Altered Refractive Development in Mice With Reduced Levels of Retinal Dopamine. Invest Ophthalmol Vis Sci 57, 4412–4419. [PubMed: 27750284]

Berson DM, Dunn FA, Takao M, 2002. Phototransduction by retinal ganglion cells that set the circadian clock. Science (New York, N.Y.) 295, 1070–1073.

Cameron MA, Pozdeyev N, Vugler AA, Cooper H, Iuvone PM, Lucas RJ, 2009. Light regulation of retinal dopamine that is independent of melanopsin phototransduction. Eur J Neurosci 29, 761–767. [PubMed: 19200071]

Cavallotti C, Pescosolido N, Artico M, Feher J, 1999. Localization of dopamine receptors in the rabbit cornea. Cornea 18, 721–728. [PubMed: 10571305]

Chakraborty R, Micic G, Thorley L, Nissen TR, Lovato N, Collins MJ, Lack LC, 2020. Myopia, or near-sightedness, is associated with delayed melatonin circadian timing and lower melatonin output in young adult humans. Sleep.

Chakraborty R, Ostrin LA, Nickla DL, Iuvone PM, Pardue MT, Stone RA, 2018. Circadian rhythms, refractive development, and myopia. Ophthalmic and Physiological Optics 38, 217–245. [PubMed: 29691928]

Chakraborty R, Pardue MT, 2015. Molecular and biochemical aspects of the retina on refraction. Progress in Molecular Biology and Translational Science.

Chakraborty R, Park H, Aung MH, Tan CC, Sidhu CS, Iuvone PM, Pardue MT, 2014. Comparison of refractive development and retinal dopamine in OFF pathway mutant and C57BL/6J wild-type mice. Mol Vis 20, 1318–1327. [PubMed: 25352740]

Chakraborty R, Park HN, Hanif AM, Sidhu CS, Iuvone PM, Pardue MT, 2015. ON pathway mutations increase susceptibility to form-deprivation myopia. Experimental eye research 137, 79–83. [PubMed: 26072023]

Chesler K, Motz C, Vo H, Douglass A, Allen RS, Feola AJ, Pardue MT, 2021. Initiation of L-DOPA Treatment After Detection of Diabetes-Induced Retinal Dysfunction Reverses Retinopathy and Provides Neuroprotection in Rats. Transl Vis Sci Technol 10, 8.

Collins M, Davis B, Wood J, 1995. Microfluctuations of steady-state accommodation and the cardiopulmonary system. Vision research 35, 2491–2502. [PubMed: 8594816]

Crosson CE, Beuerman RW, Klyce SD, 1984. Dopamine modulation of active ion transport in rabbit corneal epithelium. Invest Ophthalmol Vis Sci 25, 1240–1245. [PubMed: 6208162]

Dacey DM, Liao HW, Peterson BB, Robinson FR, Smith VC, Pokorny J, Yau KW, Gamlin PD, 2005. Melanopsin-expressing ganglion cells in primate retina signal colour and irradiance and project to the LGN. Nature 433, 749–754. [PubMed: 15716953]

Delwig A, Chaney SY, Bertke AS, Verweij J, Quirce S, Larsen DD, Yang C, Buhr E, R VANG, Gallar J, Margolis T, Copenhagen DR, 2018. Melanopsin expression in the cornea. Visual neuroscience 35, E004. [PubMed: 29905117]

Dolgin E, 2015. The myopia boom. Nature 519, 276–278. [PubMed: 25788077]

Dong F, Zhi Z, Pan M, Xie R, Qin X, Lu R, Mao X, Chen JF, Willcox MD, Qu J, Zhou X, 2011. Inhibition of experimental myopia by a dopamine agonist: different effectiveness between form deprivation and hyperopic defocus in guinea pigs. Mol Vis 17, 2824–2834. [PubMed: 22128230]

Dumitrescu ON, Pucci FG, Wong KY, Berson DM, 2009. Ectopic retinal ON bipolar cell synapses in the OFF inner plexiform layer: contacts with dopaminergic amacrine cells and melanopsin ganglion cells. The Journal of comparative neurology 517, 226–244. [PubMed: 19731338]

Ecker JL, Dumitrescu ON, Wong KY, Alam NM, Chen SK, LeGates T, Renna JM, Prusky GT, Berson DM, Hattar S, 2010. Melanopsin-expressing retinal ganglion-cell photoreceptors: cellular diversity and role in pattern vision. Neuron 67, 49–60. [PubMed: 20624591]

Erickson P, 1990. Effects of intraocular lens position errors on postoperative refractive error. Journal of cataract and refractive surgery 16, 305–311. [PubMed: 2355315]

Faulkner AE, Kim MK, Iuvone PM, Pardue MT, 2007. Head-mounted goggles for murine form deprivation myopia. J Neurosci Methods 161, 96–100. [PubMed: 17126909]

Feigl B, Zele AJ, 2014. Melanopsin-expressing intrinsically photosensitive retinal ganglion cells in retinal disease. Optometry and vision science : official publication of the American Academy of Optometry 91, 894–903. [PubMed: 24879087]

Feldkaemper M, Schaeffel F, 2013. An updated view on the role of dopamine in myopia. Experimental eye research 114, 106–119. [PubMed: 23434455]

Flitcroft DI, Harb EN, Wildsoet CF, 2020. The Spatial Frequency Content of Urban and Indoor Environments as a Potential Risk Factor for Myopia Development. Invest Ophthalmol Vis Sci 61, 42.

Grunert U, Jusuf PR, Lee SC, Nguyen DT, 2011. Bipolar input to melanopsin containing ganglion cells in primate retina. Visual neuroscience 28, 39–50. [PubMed: 20950505]

Guler AD, Ecker JL, Lall GS, Haq S, Altimus CM, Liao HW, Barnard AR, Cahill H, Badea TC, Zhao H, Hankins MW, Berson DM, Lucas RJ, Yau KW, Hattar S, 2008. Melanopsin cells are the principal conduits for rod-cone input to non-image-forming vision. Nature 453, 102–105. [PubMed: 18432195]

Hatori M, Le H, Vollmers C, Keding SR, Tanaka N, Buch T, Waisman A, Schmedt C, Jegla T, Panda S, 2008. Inducible ablation of melanopsin-expressing retinal ganglion cells reveals their central role in non-image forming visual responses. PloS one 3, e2451. [PubMed: 18545654]

Hattar S, Kumar M, Park A, Tong P, Tung J, Yau KW, Berson DM, 2006. Central projections of melanopsin-expressing retinal ganglion cells in the mouse. The Journal of comparative neurology 497, 326–349. [PubMed: 16736474]

Hattar S, Liao HW, Takao M, Berson DM, Yau KW, 2002. Melanopsin-containing retinal ganglion cells: architecture, projections, and intrinsic photosensitivity. Science (New York, N.Y.) 295, 1065–1070.

Holden BA, Fricke TR, Wilson DA, Jong M, Naidoo KS, Sankaridurg P, Wong TY, Naduvilath TJ, Resnikoff S, 2016. Global Prevalence of Myopia and High Myopia and Temporal Trends from 2000 through 2050. Ophthalmology 123, 1036–1042. [PubMed: 26875007]

Hoshi H, Liu WL, Massey SC, Mills SL, 2009. ON inputs to the OFF layer: bipolar cells that break the stratification rules of the retina. The Journal of neuroscience : the official journal of the Society for Neuroscience 29, 8875–8883. [PubMed: 19605625]

Iuvone PM, Tigges M, Fernandes A, Tigges J, 1989. Dopamine synthesis and metabolism in rhesus monkey retina: development, aging, and the effects of monocular visual deprivation. Visual neuroscience 2, 465–471. [PubMed: 2577263]

Iuvone PM, Tigges M, Stone RA, Lambert S, Laties AM, 1991. Effects of apomorphine, a dopamine receptor agonist, on ocular refraction and axial elongation in a primate model of myopia. Invest Ophthalmol Vis Sci 32, 1674–1677. [PubMed: 2016144]

Landis EG, Chrenek MA, Chakraborty R, Strickland R, Bergen M, Yang V, Iuvone PM, Pardue MT, 2020. Increased endogenous dopamine prevents myopia in mice. Experimental eye research 193, 107956. [PubMed: 32032629]

Lingham G, Mackey DA, Lucas R, Yazar S, 2020. How does spending time outdoors protect against myopia? A review. Br J Ophthalmol 104, 593–599. [PubMed: 31722876]

Lucas RJ, Hattar S, Takao M, Berson DM, Foster RG, Yau KW, 2003. Diminished pupillary light reflex at high irradiances in melanopsin-knockout mice. Science (New York, N.Y.) 299, 245–247.

Mao J, Liu S, Qin W, Li F, Wu X, Tan Q, 2010. Levodopa inhibits the development of form-deprivation myopia in guinea pigs. Optometry and vision science : official publication of the American Academy of Optometry 87, 53–60. [PubMed: 19901858]

Matynia A, Parikh S, Deot N, Wong A, Kim P, Nusinowitz S, Gorin M.B.J.E.e.r., 2015. Light aversion and corneal mechanical sensitivity are altered by intrinscally photosensitive retinal ganglion cells in a mouse model of corneal surface damage. 137, 57–62.

McBrien NA, Cottriall CL, Annies R, 2001. Retinal acetylcholine content in normal and myopic eyes: a role in ocular growth control? Visual neuroscience 18, 571–580. [PubMed: 11829303]

McCarthy CS, Megaw P, Devadas M, Morgan IG, 2007. Dopaminergic agents affect the ability of brief periods of normal vision to prevent form-deprivation myopia. Experimental eye research 84, 100–107. [PubMed: 17094962]

Morgan IG, 2003. The biological basis of myopic refractive error. Clinical & experimental optometry : journal of the Australian Optometrical Association 86, 276–288.

Morgan IG, French AN, Ashby RS, Guo X, Ding X, He M, Rose KA, 2017. The epidemics of myopia: Aetiology and prevention. Progress in retinal and eye research.

Morgan IG, Ohno-Matsui K, Saw SM, 2012. Myopia. Lancet 379, 1739–1748. [PubMed: 22559900]

Munteanu T, Noronha KJ, Leung AC, Pan S, Lucas JA, Schmidt TM, 2018. Light-dependent pathways for dopaminergic amacrine cell development and function. Elife 7.

Mutti DO, Mitchell GL, Moeschberger ML, Jones LA, Zadnik K, 2002. Parental myopia, near work, school achievement, and children's refractive error. Invest Ophthalmol Vis Sci 43, 3633–3640. [PubMed: 12454029]

Nir I, Haque R, Iuvone PM, 2000. Diurnal metabolism of dopamine in the mouse retina. Brain research 870, 118–125. [PubMed: 10869508]

Panda S, Sato TK, Castrucci AM, Rollag MD, DeGrip WJ, Hogenesch JB, Provencio I, Kay SA, 2002. Melanopsin (Opn4) requirement for normal light-induced circadian phase shifting. Science (New York, N.Y.) 298, 2213–2216.

Pardue MT, Faulkner AE, Fernandes A, Yin H, Schaeffel F, Williams RW, Pozdeyev N, Iuvone PM, 2008. High susceptibility to experimental myopia in a mouse model with a retinal on pathway defect. Invest Ophthalmol Vis Sci 49, 706–712. [PubMed: 18235018]

Pardue MT, Stone RA, Iuvone PM, 2013. Investigating mechanisms of myopia in mice. Experimental eye research 114, 96–105. [PubMed: 23305908]

Park H, Qazi Y, Tan C, Jabbar SB, Cao Y, Schmid G, Pardue MT, 2012. Assessment of axial length measurements in mouse eyes. Optometry and vision science : official publication of the American Academy of Optometry 89, 296–303. [PubMed: 22246334]

Park HN, Jabbar SB, Tan CC, Sidhu CS, Abey J, Aseem F, Schmid G, Iuvone PM, Pardue MT, 2014. Visually-driven ocular growth in mice requires functional rod photoreceptors. Invest Ophthalmol Vis Sci 55, 6272–6279. [PubMed: 25183765]

Prigge CL, Yeh PT, Liou NF, Lee CC, You SF, Liu LL, McNeill DS, Chew KS, Hattar S, Chen SK, Zhang DQ, 2016. M1 ipRGCs Influence Visual Function through Retrograde Signaling in the Retina. The Journal of neuroscience : the official journal of the Society for Neuroscience 36, 7184–7197. [PubMed: 27383593]

Rohrer B, Spira AW, Stell WK, 1993. Apomorphine blocks form-deprivation myopia in chickens by a dopamine D2-receptor mechanism acting in retina or pigmented epithelium. Visual neuroscience 10, 447–453. [PubMed: 8494798]

Rose KA, Morgan IG, Ip J, Kifley A, Huynh S, Smith W, Mitchell P, 2008. Outdoor activity reduces the prevalence of myopia in children. Ophthalmology 115, 1279–1285. [PubMed: 18294691]

Ruby NF, Brennan TJ, Xie X, Cao V, Franken P, Heller HC, O'Hara BF, 2002. Role of melanopsin in circadian responses to light. Science (New York, N.Y.) 298, 2211–2213.

Sand A, Schmidt TM, Kofuji P, 2012. Diverse types of ganglion cell photoreceptors in the mammalian retina. Progress in retinal and eye research 31, 287–302. [PubMed: 22480975]

Sankaridurg P, Tahhan N, Kandel H, Naduvilath T, Zou H, Frick KD, Marmamula S, Friedman DS, Lamoureux E, Keeffe J, Walline JJ, Fricke TR, Kovai V, Resnikoff S, 2021. IMI Impact of Myopia. Invest Ophthalmol Vis Sci 62, 2.

Saw S, 2006. How blinding is pathological myopia? BMJ Publishing Group Ltd.

Schaeffel F, 2008. Test systems for measuring ocular parameters and visual function in mice. Front Biosci 13, 4904–4911. [PubMed: 18508555]

Schaeffel F, Burkhardt E, Howland HC, Williams RW, 2004. Measurement of refractive state and deprivation myopia in two strains of mice. Optometry and vision science : official publication of the American Academy of Optometry 81, 99–110. [PubMed: 15127929]

Schmid KL, Wildsoet CF, 1997. Contrast and spatial-frequency requirements for emmetropization in chicks. Vision research 37, 2011–2021. [PubMed: 9327048]

Schmidt TM, Alam NM, Chen S, Kofuji P, Li W, Prusky GT, Hattar S, 2014. A role for melanopsin in alpha retinal ganglion cells and contrast detection. Neuron 82, 781–788. [PubMed: 24853938]

Schmidt TM, Chen SK, Hattar S, 2011a. Intrinsically photosensitive retinal ganglion cells: many subtypes, diverse functions. Trends in neurosciences 34, 572–580. [PubMed: 21816493]

Schmidt TM, Do MT, Dacey D, Lucas R, Hattar S, Matynia A, 2011b. Melanopsin-positive intrinsically photosensitive retinal ganglion cells: from form to function. The Journal of neuroscience : the official journal of the Society for Neuroscience 31, 16094–16101. [PubMed: 22072661]

Schmidt TM, Kofuji P, 2011. Structure and function of bistratified intrinsically photosensitive retinal ganglion cells in the mouse. The Journal of comparative neurology 519, 1492–1504. [PubMed: 21452206]

Schmucker C, Schaeffel F, 2004a. In vivo biometry in the mouse eye with low coherence interferometry. Vision research 44, 2445–2456. [PubMed: 15358080]

Schmucker C, Schaeffel F, 2004b. A paraxial schematic eye model for the growing C57BL/6 mouse. Vision research 44, 1857–1867. [PubMed: 15145680]

Stone RA, Lin T, Laties AM, Iuvone PM, 1989. Retinal dopamine and form-deprivation myopia. Proc Natl Acad Sci U S A 86, 704–706. [PubMed: 2911600]

Stone RA, McGlinn AM, Baldwin DA, Tobias JW, Iuvone PM, Khurana TS, 2011a. Image defocus and altered retinal gene expression in chick: clues to the pathogenesis of ametropia. Invest Ophthalmol Vis Sci 52, 5765–5777. [PubMed: 21642623]

Stone RA, McGlinn AM, Baldwin DA, Tobias JW, Iuvone PM, Khurana T.S.J.I.o., science, v., 2011b. Image defocus and altered retinal gene expression in chick: clues to the pathogenesis of ametropia. 52, 5765–5777.

Stone RA, McGlinn AM, Chakraborty R, Lee DC, Yang V, Elmasri A, Landis E, Shaffer J, Iuvone PM, Zheng X, Sehgal A, Pardue MT, 2019. Altered ocular parameters from circadian clock gene disruptions. PloS one 14, e0217111–e0217111. [PubMed: 31211778]

Stone RA, Pardue MT, Iuvone PM, Khurana TS, 2013. Pharmacology of myopia and potential role for intrinsic retinal circadian rhythms. Experimental eye research 114, 35–47. [PubMed: 23313151]

Stone RA, Wei W, Sarfare S, McGeehan B, Engelhart KC, Khurana TS, Maguire MG, Iuvone PM, Nickla DL, 2020. Visual Image Quality Impacts Circadian Rhythm-Related Gene Expression in Retina and in Choroid: A Potential Mechanism for Ametropias. Invest Ophthalmol Vis Sci 61, 13.

Storch K-F, Paz C, Signorovitch J, Raviola E, Pawlyk B, Li T, Weitz CJ, 2007. Intrinsic circadian clock of the mammalian retina: importance for retinal processing of visual information. Cell 130, 730–741. [PubMed: 17719549]

Thomson K, Karouta C, Morgan I, Kelly T, Ashby R, 2019. Effectiveness and safety of topical levodopa in a chick model of myopia. Scientific Reports 9, 18345. [PubMed: 31797988]

Thomson K, Morgan I, Karouta C, Ashby R, 2020. Levodopa inhibits the development of lens-induced myopia in chicks. Scientific Reports 10, 13242. [PubMed: 32764736]

Tosini G, Pozdeyev N, Sakamoto K, Iuvone PM, 2008. The circadian clock system in the mammalian retina. Bioessays 30, 624–633. [PubMed: 18536031]

Troilo D, Smith EL 3rd, Nickla DL, Ashby R, Tkatchenko AV, Ostrin LA, Gawne TJ, Pardue MT, Summers JA, Kee CS, Schroedl F, Wahl S, Jones L, 2019. IMI - Report on Experimental Models of Emmetropization and Myopia. Invest Ophthalmol Vis Sci 60, M31–m88. [PubMed: 30817827]

Turner PV, Albassam MA, 2005. Susceptibility of rats to corneal lesions after injectable anesthesia. Comparative medicine 55, 175–182. [PubMed: 15884781]

Vugler AA, Redgrave P, Semo M, Lawrence J, Greenwood J, Coffey PJ, 2007. Dopamine neurones form a discrete plexus with melanopsin cells in normal and degenerating retina. Experimental neurology 205, 26–35. [PubMed: 17362933]

Witkovsky P, 2004. Dopamine and retinal function. Documenta ophthalmologica. Advances in ophthalmology 108, 17–40. [PubMed: 15104164]

Wu PC, Huang HM, Yu HJ, Fang PC, Chen CT, 2016. Epidemiology of Myopia. Asia-Pacific journal of ophthalmology (Philadelphia, Pa.) 5, 386–393.

Zele AJ, Feigl B, Adhikari P, Maynard ML, Cao D, 2018. Melanopsin photoreception contributes to human visual detection, temporal and colour processing. Scientific Reports 8, 3842. [PubMed: 29497109]

Zhang DQ, Belenky MA, Sollars PJ, Pickard GE, McMahon DG, 2012. Melanopsin mediates retrograde visual signaling in the retina. PloS one 7, e42647. [PubMed: 22880066]

Zhang DQ, Wong KY, Sollars PJ, Berson DM, Pickard GE, McMahon DG, 2008. Intraretinal signaling by ganglion cell photoreceptors to dopaminergic amacrine neurons. Proc Natl Acad Sci U S A 105, 14181–14186. [PubMed: 18779590]

Zhao X, Wong KY, Zhang DQ, 2017. Mapping physiological inputs from multiple photoreceptor systems to dopaminergic amacrine cells in the mouse retina. Sci Rep 7, 7920. [PubMed: 28801634]

Zheng W, Chen Y, Zhou X, Zhang X, Chen Y, Guan X, Mao J, 2020. Regulation of Retinal Melanopsin on Lens-induced Myopia in Guinea Pigs. Optometry and vision science : official publication of the American Academy of Optometry 97, 489–495. [PubMed: 32697555]

Zhou X, Pardue MT, Iuvone PM, Qu J, 2017. Dopamine signaling and myopia development: What are the key challenges. Progress in retinal and eye research 61, 60–71. [PubMed: 28602573]

Highlights

- Dysfunction in retinal melanopsin signaling alters refractive development in mice
- Form-deprivation (FD) myopia is enhanced with disrupted melanopsin signaling
- Retinal dopamine signaling is reduced in form-deprived mice lacking melanopsin
- Systemic L-DOPA treatment attenuates FD myopia in melanopsin knockout mice
- Melanopsin is vital for refractive development and slowing myopia progression

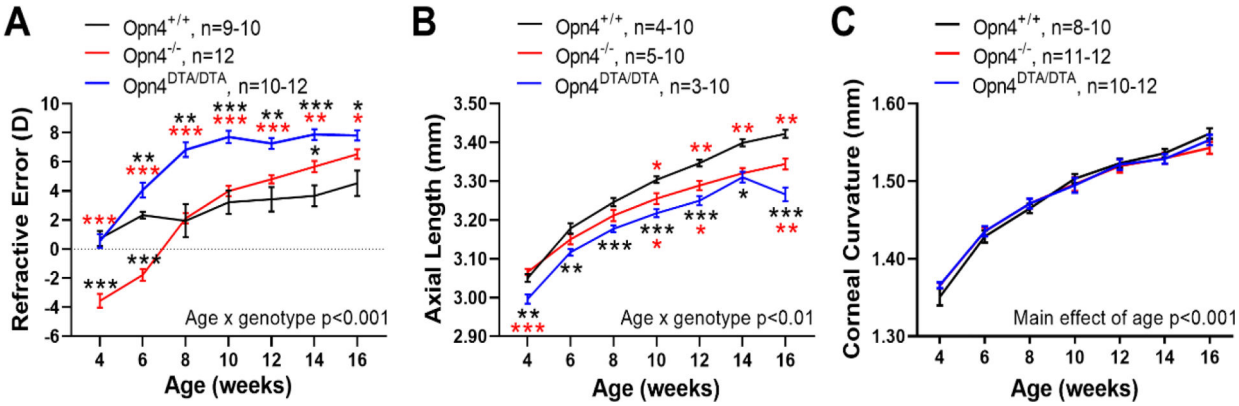

Figure 1.

Loss of melanopsin alters refractive development and ocular growth. A) Refractive error measurements in *Opn4*$^{+/+}$ (black), *Opn4*$^{-/-}$ (red), and *Opn4*$^{DTA/DTA}$ (blue) mice. *Opn4*$^{-/-}$ mice had a steeper refractive development curve (p<0.001) that led to hyperopia compared to *Opn4*$^{+/+}$ mice, with significantly more myopic refractions at earlier ages (p<0.001) and hyperopic refractions at older ages. *Opn4*$^{DTA/DTA}$ showed significantly more hyperopic refractions than the other two genotypes (p<0.001). B) Shorter axial length (p<0.001) in *Opn4*$^{-/-}$ mice compared to *Opn4*$^{+/+}$ at later ages. *Opn4*$^{DTA/DTA}$ mice also had significantly shorter axial lengths than *Opn4*$^{+/+}$ or *Opn4*$^{-/-}$ mice across most ages (p<0.001). C) Corneal curvature was not different between *Opn4*$^{+/+}$, *Opn4*$^{-/-}$, and *Opn4*$^{DTA/DTA}$ mice (p=0.98) but increased with age (p<0.001). Data are presented as mean ± SEM. Comparisons were performed with RM two-way mixed-effects analysis (MEA) with Holm-Sidak multiple comparisons tests (HSK) where *p<0.05, **p<0.01, and ***p<0.001. Black and red asterisks = significant differences compared to *Opn4*$^{+/+}$ and *Opn4*$^{-/-}$ mice, respectively.

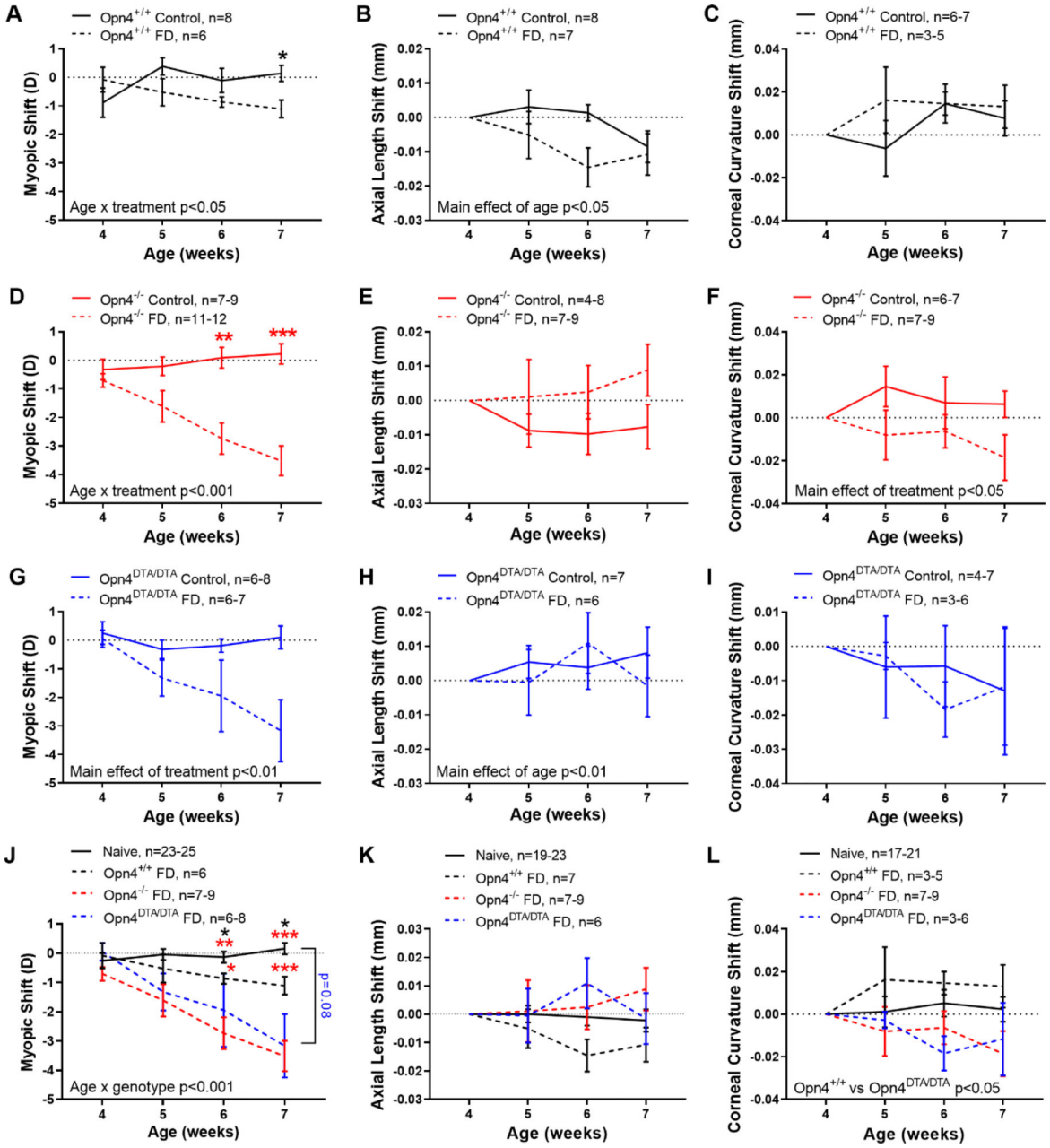

Figure 2.

Larger response to form-deprivation (FD) in melanopsin deficient mice. A) FD caused a myopic shift in *Opn4*$^{+/+}$ (solid line) mice after 3 weeks (dashed line, p<0.05). B) There was no effect of FD on axial length in *Opn4*$^{+/+}$ mice, but the axial length shift changed with age (p<0.05) C). Corneal curvature did not significantly change with FD. D-F) Same as in A-B but for *Opn4*$^{-/-}$ mice. There was a significant myopic shift with FD (p<0.001) but no change in axial length. However, cornea radii became shorter in the FD eye (p<0.05), developing a steeper corneal curvature. G-I) Same as in A-B but for *Opn4*$^{DTA/DTA}$ mice. FD led to a significant myopic shift (p<0.01) but no change in axial length or corneal curvature. J) Myopic shifts compared between naïve (solid black), *Opn4*$^{+/+}$ FD (dashed black), *Opn4*$^{-/-}$

FD (dashed red), and *Opn4*$^{DTA/DTA}$ FD (dashed blue) mice. *Opn4*$^{+/+}$ (black), *Opn4*$^{-/-}$ (red), and *Opn4*$^{DTA/DTA}$ (blue) mice. *Opn4*$^{-/-}$ mice show significantly greater susceptibility to FD than *Opn4*$^{+/+}$ mice ($p<0.001$) and both *Opn4*$^{-/-}$ and *Opn4*$^{DTA/DTA}$ mice responded similarly to FD ($p=0.34$). Black and red asterisks denote significance between naïve compared to *Opn4*$^{+/+}$ and *Opn4*$^{-/-}$ mice, respectively. K) There was no difference in axial length shift across genotypes. L) Corneal curvature after FD was only significantly different between *Opn4*$^{+/+}$ and *Opn4*$^{DTA/DTA}$ mice ($p=0.03$). Axial length and corneal curvature values were normalized to 4 weeks of age. Data are presented as mean ± SEM. Comparisons between treatment (FD vs control) and genotypes were performed with MEA (or ANOVA) with HSK where *$p<0.05$, **$p<0.01$, and ***$p<0.001$.

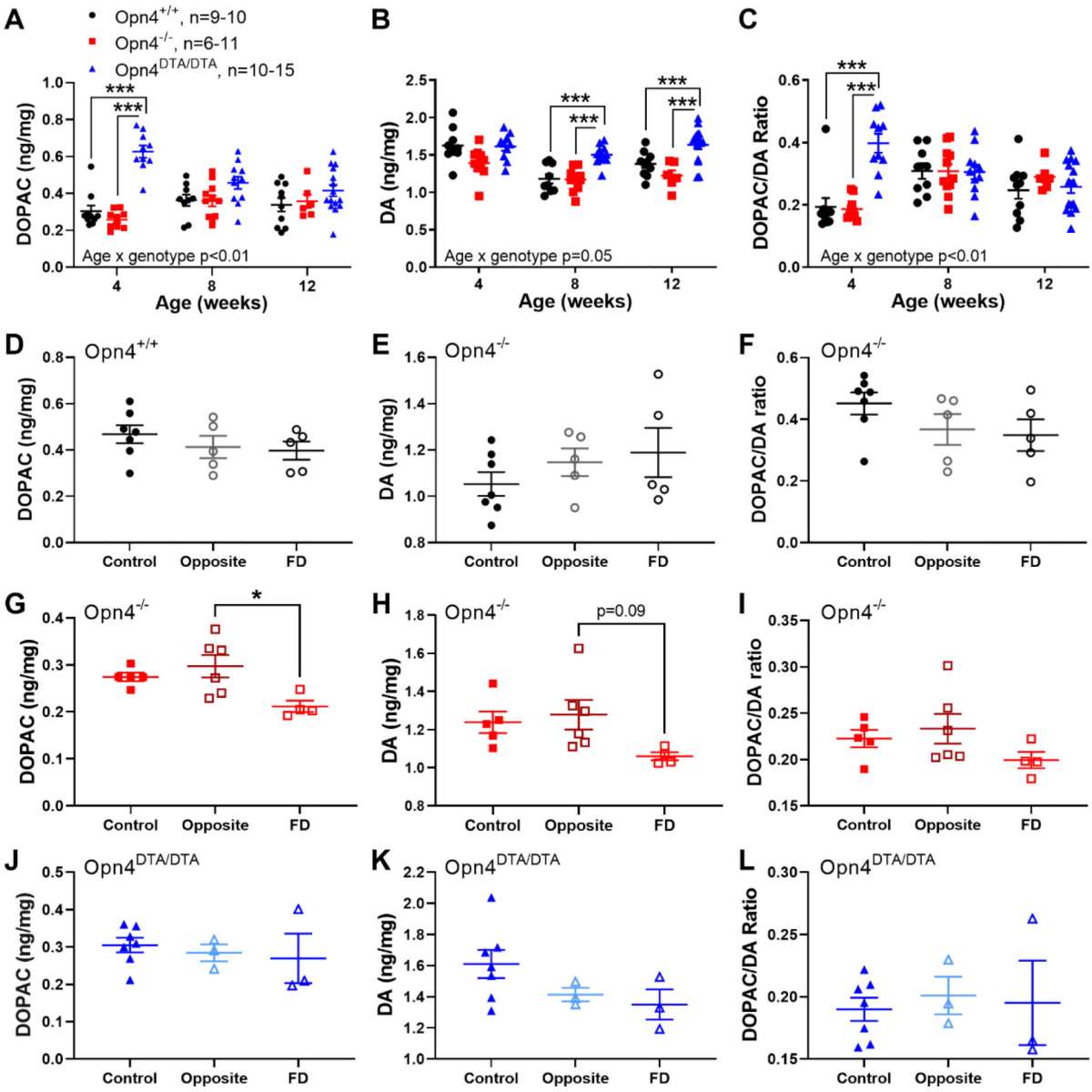

Figure 3.

Altered retinal DA and DOPAC levels in normal and FD eyes in the absence of melanopsin. A-C) DOPAC (A), DA (B), and the DOPAC/DA ratio (C) values for *Opn4*$^{+/+}$ (black), *Opn4*$^{-/-}$ (red), and *Opn4*$^{DTA/DTA}$ mice (blue) across age. For *Opn4*$^{+/+}$ and *Opn4*$^{-/-}$ mice, DOPAC levels increased (A, $p<0.05$) and DA levels decreased (B, $p<0.001$) from 4 to 12 weeks, which was also reflected in the increased DOPAC/DA ratio after 4 weeks (C, $p<0.001$). In *Opn4*$^{DTA/DTA}$ mice, DOPAC levels were significantly higher at 4 weeks (A) and DA levels were significantly higher at 8 and 12 weeks (B) than in the other mice. However, the DOPAC/DA ratio was only higher in *Opn4*$^{DTA/DTA}$ mice at 4 weeks (C). D-E) In *Opn4*$^{+/+}$ mice, 3 weeks of FD did not alter DOPAC (D), DA (E), or the DOPAC/DA ratio (F) between control (solid dark symbols, n=5), opposite (open light symbols, n=6), or FD eyes (open dark symbols, n=4). G-I) In *Opn4*$^{-/-}$ mice, FD eyes (n=5) had significantly

lower DOPAC levels than the opposite eyes (n=5, $p<0.05$, G) but not the control eyes (n=7). A similar trend was seen with DA (H) but not with the DOPAC/DA ratio (I). J-L) In *Opn4*$^{DTA/DTA}$ mice, there was no difference in DOPAC (J), DA (K), or the DOPAC/DA ratio (L) between control (n=7), opposite (n=3), or FD (n=3) mice. Data are presented as mean ± SEM. Comparisons were performed with MEA (A-C) and one-way ANOVA (D-L), both with HSK where *$p<0.05$ and ***$p<0.001$.

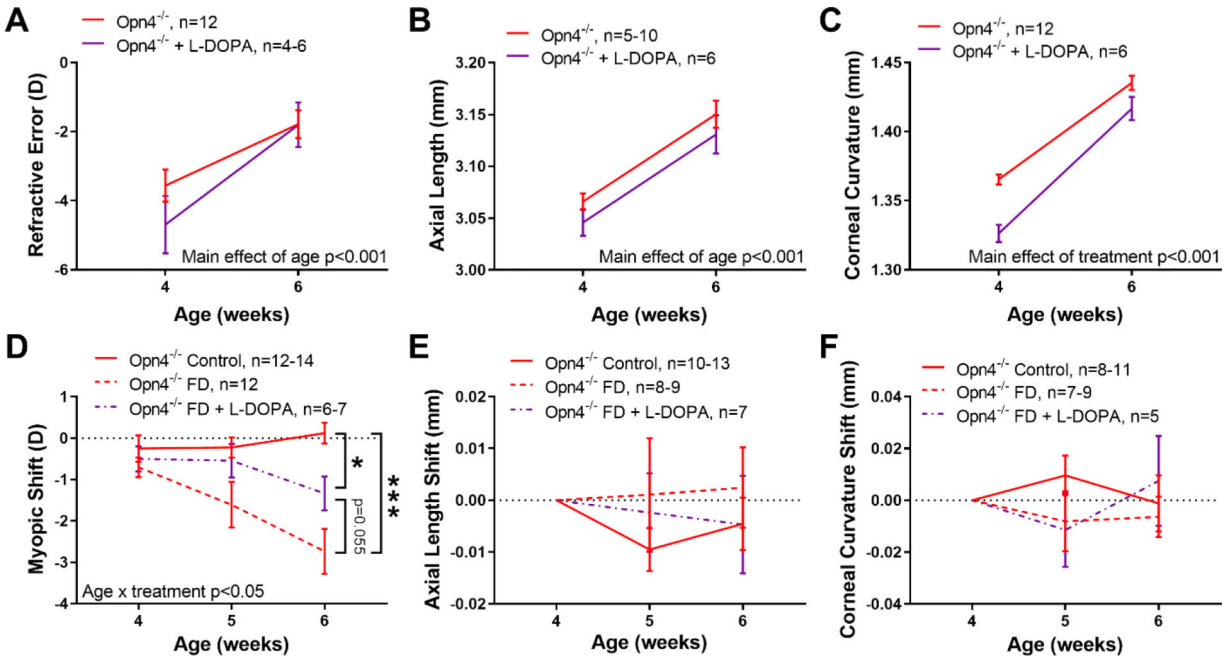

Figure 4.

L-DOPA attenuates FD myopia. A) L-DOPA treatment (purple) did not prevent spontaneous myopia in *Opn4*$^{-/-}$ mice compared to control (red). L-DOPA treatment caused significantly steeper corneal curvature than control mice (C) but no change in axial length (B). D) Myopic shifts in FD *Opn4*$^{-/-}$ mice treated with L-DOPA (purple dashed lines) were less myopic compared to FD *Opn4*$^{-/-}$ (red dashed lines, p=0.055) but still had greater myopic shifts than *Opn4*$^{-/-}$ controls. E-F) L-DOPA treatment with FD did not cause significant changes in axial length or corneal curvature in *Opn4*$^{-/-}$ mice. Data are presented as mean ± SEM. Comparisons were performed in A-B, D-F with MEA and C with ANOVA, both with HSK where *p<0.05 and ***p<0.001.

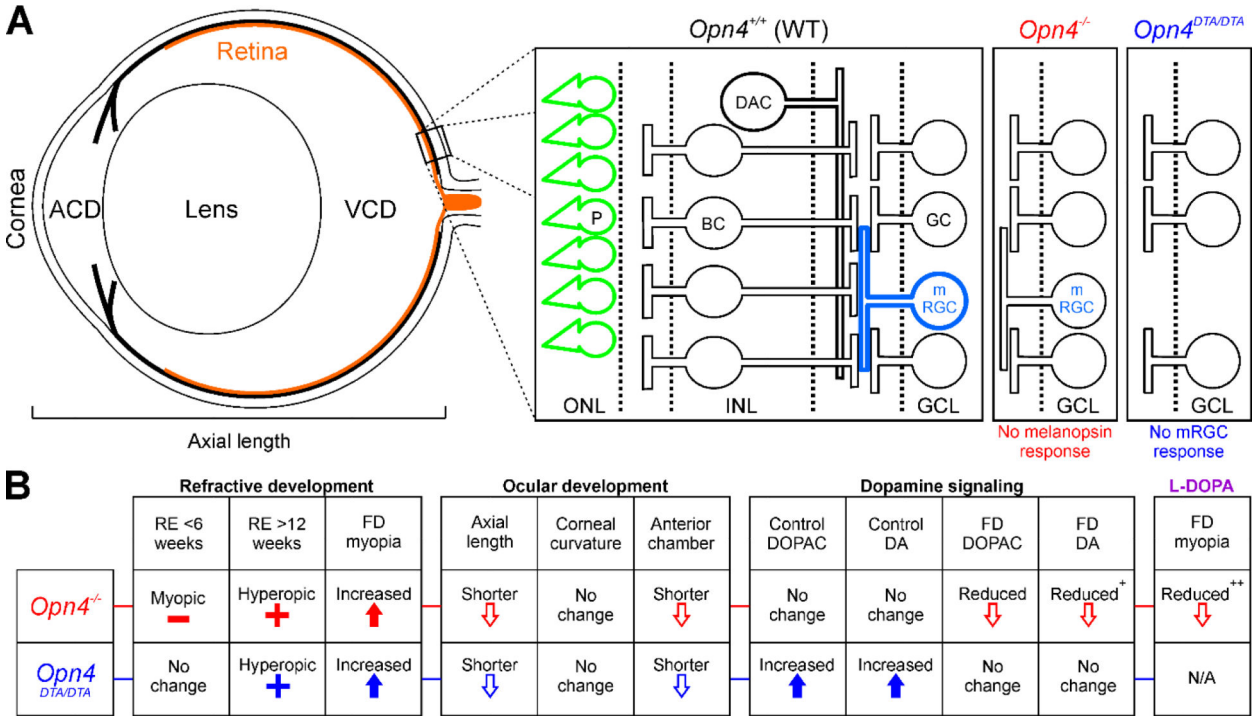

Figure 5.

Major development and signaling changes in the absence of melanopsin. A) Schematic of the mouse eye showing the major ocular development parameters (left, ACD = anterior chamber depth, VCD = vitreous chamber depth) and the major retinal pathways associated with melanopsin-mediated signaling (right). In *Opn4*$^{+/+}$ mice, both photoreceptors (P, green) and mRGCs (light blue) directly detect light. mRGCs also receive photoreceptor-mediated synaptic input through bipolar cells (BC) and have interactions with dopaminergic pathways (DAC). In *Opn4*$^{-/-}$ mice (red), mRGCs still respond to light through photoreceptor-mediated synaptic signaling but no longer have intrinsic melanopsin light responses. In *Opn4*$^{DTA/DTA}$ mice (blue), mRGCs are not present and the retina loses both intrinsic mRGC and synaptic melanopsin responses. B) Summary table of the effects of melanopsin signaling disruption on refractive development, ocular development, and dopamine signaling. RE = refractive error. FD = form-deprivation. DA = dopamine. All parameters are in comparison to *Opn4*$^{+/+}$ or the un-treated condition. + indicates $p<0.10$. ++ indicates $p<0.10$ in comparison to *Opn4*$^{-/-}$ mice without L-DOPA treatment.